Electronic Supplementary Material (ESI) for Journal of Materials Chemistry C.

Supplementary information for:

$In_{0.5}Ga_{0.5}N$ by Atomic Layer Deposition

Polla Rouf, Justinas Palisaitis, Babak Bakhit, Nathan J. O'Brien, Henrik Pedersen*

Department of Physics, Chemistry and Biology, Linköping University, SE-58183 Linköping, Sweden

** E-mail: polla.rouf@liu.se*

Contents of the supplementary information:

Experimental details

*Caution! As catenated nitrogen compounds are known to be associated with explosive hazards, isopropylazide and compounds **1** and **2** are possible explosive energetic materials. Although we have not experienced any difficulties or problems in the synthesis, characterization, sublimation and handling of compounds **1** and **2**, its energetic properties have not been investigated and are therefore unknown. We therefore highly recommend all appropriate standard safety precautions for handling explosive materials (safety glasses, face shield, blast shield, leather gloves, polymer apron and ear protection) be used at all times when working with isopropylazide and compounds **1** and **2**.*

Precursor synthesis

Tris(1,3-diisopropyltriazenide)indium(III) (**1**) and tris(1,3-diisopropyltriazenide)gallium(III) (**2**) were synthesized according to the literature procedures.[1,2] The reactions and handling of the precursors were undertaken in a dry nitrogen atmosphere on a Schlenk line and in a glove box (GS Gloveboxsystemtechnik). The precursor powders were mixed by a filling a glass vial with **1** and **2** to a total weight of ~1.0 g and further mixed by a spoon to obtain a uniform mixture. The glass vial was placed in a stainless-steel container and inserted in a heated sublimator in the ALD reactor.

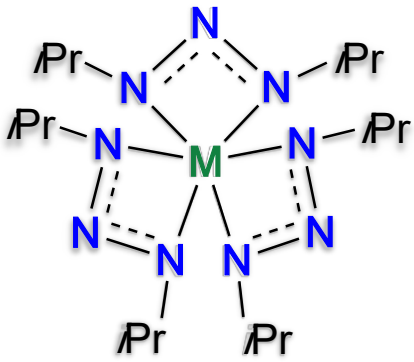

Figure S1: *Schematic illustration of the tris(1,3-diisopropyltriazenide)indium (III) and gallium (III) precursors where M indicates the metals (In and Ga).*

Film deposition

A hot-wall Picosun R-200 ALD reactor, equipped with a Litmas remote ICP plasma source, was used for the deposition. The reactor operated at 4 mbar with a continuous flow of high purity N_2 (99,999% with further drying using a getter filter) into the chamber, which was also

used as the purge gas. The reactor was baked at 450 °C for 2 hours with a 300 sccm flow of N_2 to remove traces of H_2O and O_2 in the deposition chamber due to exposure of the deposition chamber to the atmosphere during substrate exchange as no load-lock chamber was used. The precursor mixture was sublimed at 130 °C if nothing else is stated. An amount of ~1.0 g of precursor mixture was enough for 1000 cycles and the amount of precursor required increased linearly with the number of cycles. NH_3 plasma was used as the nitrogen precursor. A gas mixture flow of 100 sccm Ar (99.999% and further purified by a getter filter) and 75 sccm NH_3 (AGA/Linde, 99.999% and further purified by a getter filter) was ignited by 2800 W plasma power. The ICP plasma source was located approximately 75 cm above the substrate. Unless otherwise stated, a 12s NH_3 plasma and a 10s N_2 purge after both metal pulse and plasma pulse was used. Si(100) and 4H-SiC wafers were cut into 15 x 15 mm^2 pieces and used as substrates in this study. Prior to deposition, the 4H-SiC pieces were cleaned with RCA-1 (1:1:5 solution of H_2O_2 (30%), NH_3 (25%) and H_2O) and RCA-2 (1:1:6 solution of H_2O_2 (30%), HCl (37%) and H_2O) solutions to remove organic and inorganic contaminants. The Si(100) pieces were used without further *ex situ* cleaning.

Film characterization

Film thickness was measured by X-ray reflectivity (XRR) and film crystallinity was measured by X-ray diffraction (XRD) in θ-2θ mode using an PANalytical X'Pert PRO with a Cu-anode tube and Bragg-Brentano HD optics. To analyze the thickness, the software PANalytical X'Pert reflectivity and a two-layer model was used to fit the data, InGaN/substrate. PANalytical EMPYREAN MRD XRD with a Cu-anode X-ray tube and 5-axis (x-y-z-v-u) sample stage operating at 45 kV and 40 mA was used for the pole figures measurement using an X-ray lens and parallel plate collimator. Elemental compositions were obtained using XPS , RBS and ToF-ERDA. Kratos AXIS Ultra DLD X-ray photoelectron spectroscopy (XPS) equipped with Ar sputtering was used. The film composition was collected after Ar sputtering for 600 s with a beam energy of 0.5 keV with a sputtering area of 3 mm^2. The RBS and ToF-ERDA measurements were carried out in a 5-MV NEC-5SDH-2 pelletron tandem accelerator. RBS employed 2 MeV $^4He^+$ ions and detected in a scattering angle of 170°. Two different geometries, azimuth angles of 5°+tilt angle 2° and 40°+tilt angle 2°, were chosen to minimize channeling effects. In addition, suppression of the probable channeling effects was undertaken by multiple small random-angular movements around the equilibrium angles within a range of 2°. RBS spectra was fitted by SIMNRA 7.02 code[3] with an ~1% statistic uncertainty to determine elemental compositions. In ToF-ERDA, recoils were detected at 45° angle between

the primary beam and a ToF-E detector telescope in a gas ionization chamber (GIC) using a 36 MeV $^{127}I^{8+}$ beam incident at 67.5° with respect to the sample surface normal. The ToF-E detector telescope consists of two circular carbon foils with 8 and 5 μg/cm^2 thicknesses, 6 mm radius, a 0.05-msr solid angle (ΔΩ), and a flight distance of 425 mm between the foils. Utilizing a ToF-GIC setup provides a system with a good energy resolution and enhanced ion species separation in terms of mass and energy.[4] Average elemental compositions was also obtained from ToF-ERDA time-energy coincidence spectra using two different software packages, CONTES[5] and Potku[6]. Systematic uncertainties of the experiment, discussed in more detail elsewhere[7] in particular for light elements, was estimated to be maximum 5-10%, whereas statistic uncertainties arisen from the number of experimental counts was < 2.3%. However, the relative elemental concentrations was obtained with higher accuracy.[8,9] The stopping power data required for both RBS and ERDA simulations was retrieved from SRIM2013 code.[10] Cross-sectional transmission electron microscope (TEM) samples were prepared by the traditional sandwich approach, which includes sample cutting, gluing, polishing and ion milling. A Gatan Precision Ion Polishing System Model 691 operated at 5kV and 40 mA, with an Ar ion source, was used to make the samples electron transparent. Scanning transmission electron microscopy (STEM), selective area electron diffraction (SAED), energy dispersive X-ray analysis (EDX) and electron energy loss spectroscopy (EELS) characterization were performed using the Linköping double Cs corrected FEI Titan^3 60-300, operated at 300 kV. The absorbance measurements were conducted using a custom fiber optical setup consisting of a light source (Ocean Optics DH-2000-BAL), a detector (Avantes AvaSpec-Dual) and a bifurcated optical fiber (Ocean Optics BIFBORO-2-1000). Absorption spectra for the films were collected using a custom software based LabView (National Instruments) with a Si(100) substrate used as a reference. A LEO 1550 scanning electron microscope (SEM) with an acceleration energy of 3 kV was used to study the morphology of the film.

$In_{1-x}Ga_xN$ composition control

Deposition of $In_{1-x}Ga_xN$ was first undertaken on Si(100) substrates to investigate the co-sublimation approach where the metal precursor pulse was set to 10s. ALD of $In_{1-x}Ga_xN$ was undertaken using the same optimized parameters as our previously reported studies of InN and GaN using **1** and **2**, respectively.[1,2] Initially, the sublimation temperature was varied from 90-170°C while the deposition temperature was set to 350 °C. XPS analysis showed that the In/Ga ratio depended on the sublimation temperature (Table S1). At lower sublimation temperatures (90-120 °C), the In content was approximately twice as much as Ga. The In content increased with the deposition temperature, reaching its peak between 130-140 °C with approximately 4 times more In than Ga. The In content decreased between 150-170 °C and a near 1:1 In/Ga ratio was found for a sublimation temperature of 150 °C. The general trend is the In content of the film is always higher, however, some control of the composition can be made by changing the sublimation temperature.

XRD analysis (Fig. S2) showed that all films were crystalline except for those using a sublimation temperature of 90 °C, which gave X-ray amorphous films. The amorphous films are thought to be due to insufficient precursor delivery into the chamber. For all crystalline films, polycrystalline $In_{1-x}Ga_xN$ was observed by several diffraction peaks. For sublimation temperatures of 110 °C and 170 °C, only one peak was observed indicating a preferred growth orientation along the c-axis.

The sublimation temperature was kept constant at 130 °C while the deposition temperature was varied. XPS analysis showed the deposition temperature has a large effect on the In/Ga ratio. At lower deposition temperatures, a near 1:1 ratio of In/Ga was obtained while the In content increased drastically when increasing the deposition temperature (Table S2). The films deposited at 200 °C and 250 °C showed no peaks in the XRD measurement (Fig. S3), indicative of X-ray amorphous $In_{1-x}Ga_xN$. The films were crystalline for deposition temperatures above 350 °C, displaying several XRD peaks and indicating a polycrystalline nature or compositional difference along the growth axis.

To further evaluate the composition of the films, different ratios of **1** and **2** were mixed in the sublimator and sublimed at 130 °C for film deposition at 350 °C. Table S3 shows the mixing ratio of precursors could control the In/Ga ratio of the $In_{1-x}Ga_xN$ films when higher amounts of **1** were used. Increasing the amount of **2** showed the In/Ga ratio of the $In_{1-x}Ga_xN$ film did not follow the mixing ratio. Although higher amounts of **2** led an increase of Ga in the film. The crystallinity was not affected significantly by the mixing ratio of **1** and **2**, all rendering crystalline $In_{1-x}Ga_xN$ (Fig. S4).

As both In and Ga have a high affiliation to oxygen, avoiding surface oxidation prior to elemental analysis of the film composition was challenging. We previously capped InN with a thin layer of AlN to accurately determine the film composition with XPS.[1] A further complication with $In_{1-x}Ga_xN$ is the overlap of the Ga auger peaks with the N 1s peak in XPS.[11] This makes quantification of the overall $In_{1-x}Ga_xN$ film composition difficult and hence the reason for only comparing the metal content with each other. The elemental composition of some samples was measured with both XPS and RBS/ToF-ERDA to obtain the metal ratios from different techniques. The RBS and ToF-ERDA measurements showed the $In_{1-x}Ga_xN$ deposited at 200 °C with a sublimation temperature of 130 °C had a composition of $In_{0.47}Ga_{0.53}N$. The $In_{1-x}Ga_xN$ films deposited at 250 °C had a composition of $In_{0.50}Ga_{0.50}N$ from RBS/ERDA. XPS analysis of the films deposited at 200 °C and 250 °C showed compositions of $In_{0.52}Ga_{0.58}N$ and $In_{0.59}Ga_{0.41}N$, respectively. This shows XPS gives slightly higher In content in comparison to the ERDA measurements, which could be due to preferential sputtering.[12] In the measured films, 1 at% of carbon was also be detected. Due to long air exposure and the inability to cap the $In_{1-x}Ga_xN$ for ERDA measurements, as the nitrogen from the capping and the $In_{1-x}Ga_xN$ film cannot be distinguished, high oxygen content in the film of upwards to 20 at% was observed. Capping the $In_{1-x}Ga_xN$ would prevent post deposition oxidization and in turn drastically decrease the oxygen content, as we previously observed for InN.[1]

Table S1: *Elemental composition from XPS data of $In_{1-x}Ga_xN$ films deposited at 350 °C from a 1:1 powder ratio of **1** and **2** with different sublimation temperatures.*

Sublimation temperature (°C)	In at%	Ga at%
90	72	28
110	67	32
120	65	35
130	80	20
140	87	13
150	55	45
170	65	35

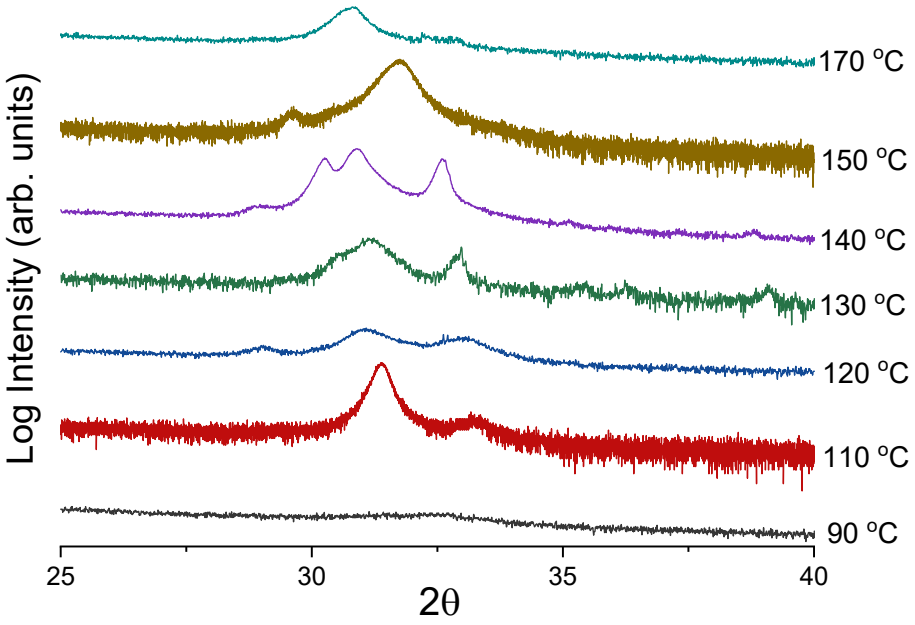

Figure S2: *θ-2θ XRD analysis of $In_{1-x}Ga_xN$ films deposited at 350 °C from a 1:1 powder ratio of **1** and **2** with different sublimation temperatures.*

Table S2: *Elemental composition from XPS data of $In_{1-x}Ga_xN$ films deposited at different temperatures from a 1:1 powder ratio of **1** and **2** sublimed at 130 °C.*

Deposition temperature (°C)	In at%	Ga at%
200	52	48
250	59	41
350	80	20
380	98	2
400	90	10

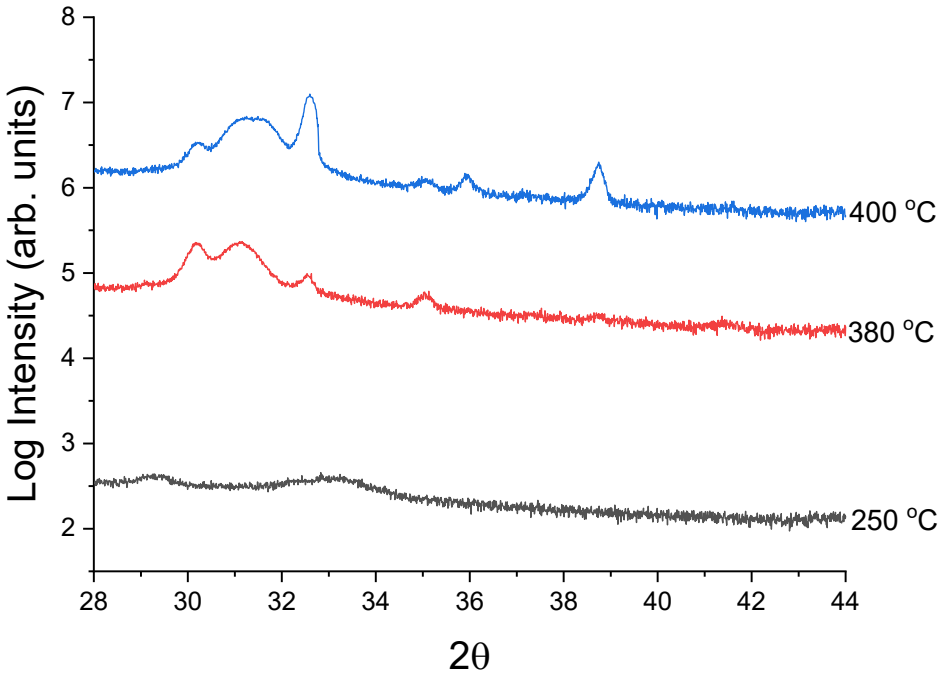

Figure S3: *θ-2θ XRD analysis of $In_{1-x}Ga_xN$ films deposited at different temperatures from a 1:1 powder ratio of **1** and **2** sublimed at 130 °C.*

Table S3: *Elemental composition from XPS data of $In_{1-x}Ga_xN$ films deposited at 350 °C with different mixing ratios of **1** and **2** sublimed at 130 °C.*

Mixing ratio 1	2	In at%	Ga at%
9	1	99	1
7	3	72	28
1	1	80	20
3	7	71	29
1	9	52	48

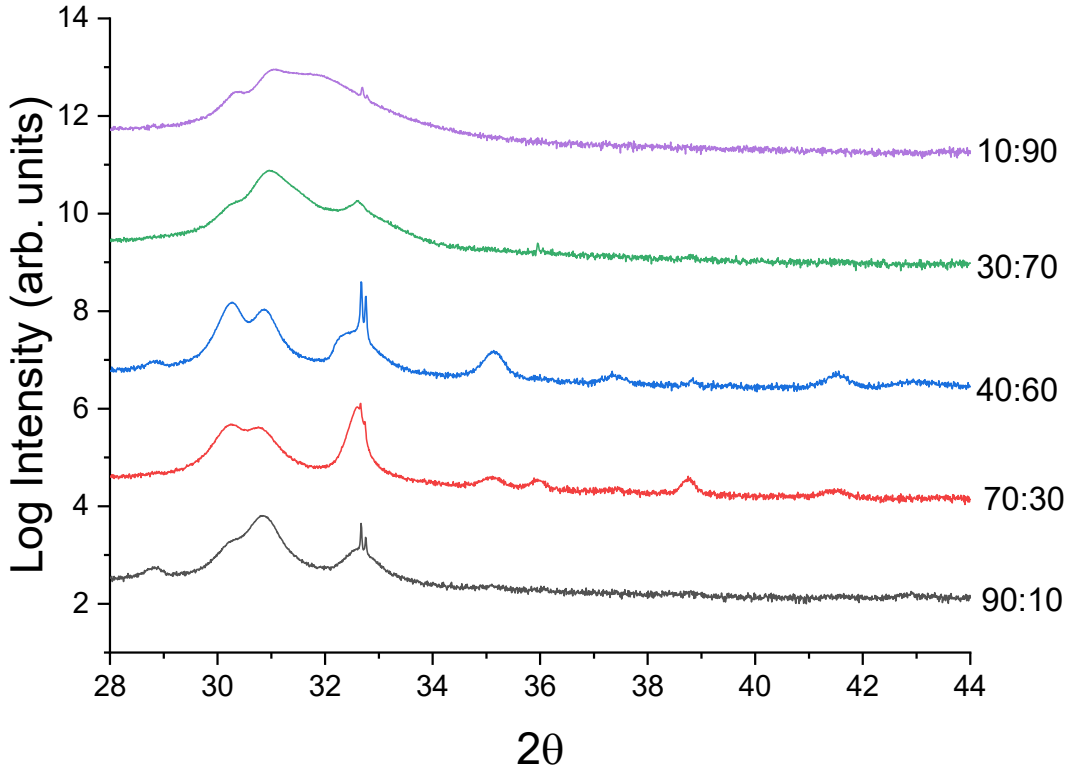

Figure S4: *θ-2θ XRD analysis of $In_{1-x}Ga_xN$ films deposited at 350 °C with different mixing ratios of **1** and **2** sublimed at 130 °C.*

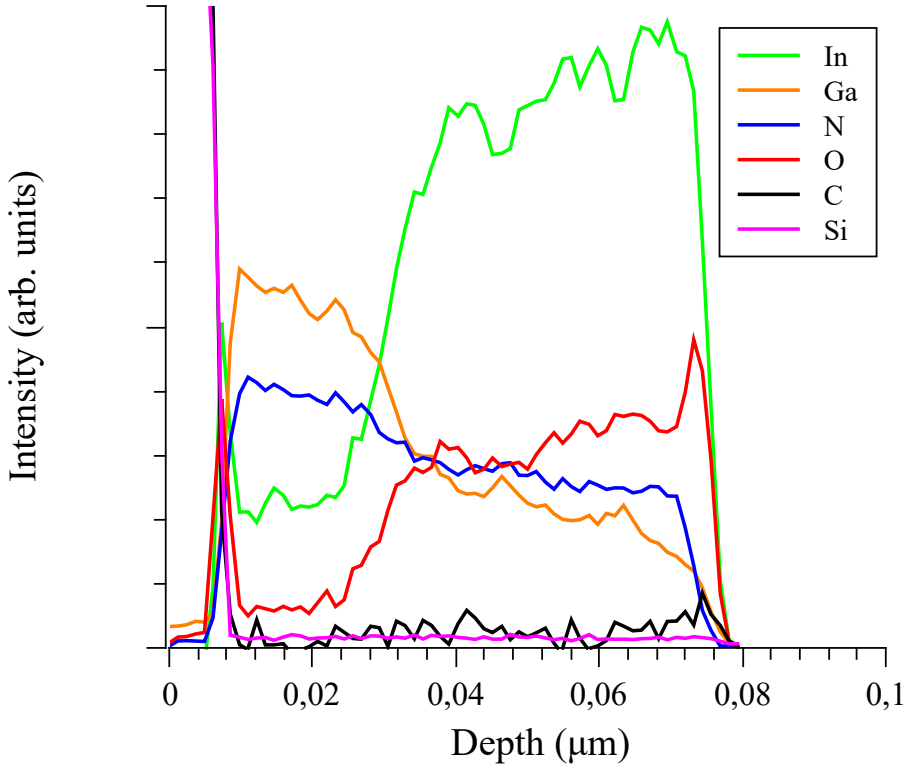

Figure S5: *EDX line profile obtained in TEM of epitaxial $In_xGa_{1-x}N$ deposited at 350 °C from a 1:1 powder ratio of* ***1*** *and* ***2*** *sublimed at 130 °C.*

Valence (V)EELS analysis was employed by examining the low-loss EELS region to evaluate the bulk plasmon peak positions from two distinct regions of the epitaxial film deposited on 4H-SiC(0001) (closer to substrate and top of the film), Fig. S5. The position of the bulk plasmon peaks were estimated to be ~18.7 eV near the interface and ~16.2 eV closer to the top of the InGaN film. Pure InN and GaN have plasmon peak at 15.5 eV and 19.4 eV, respectively.[13] By following the linear dependence between binaries the composition of ternary alloy could be extracted giving $In_{18}Ga_{82}N$ near the interface and $In_{82}Ga_{18}N$ close to the top, respectively.[14]

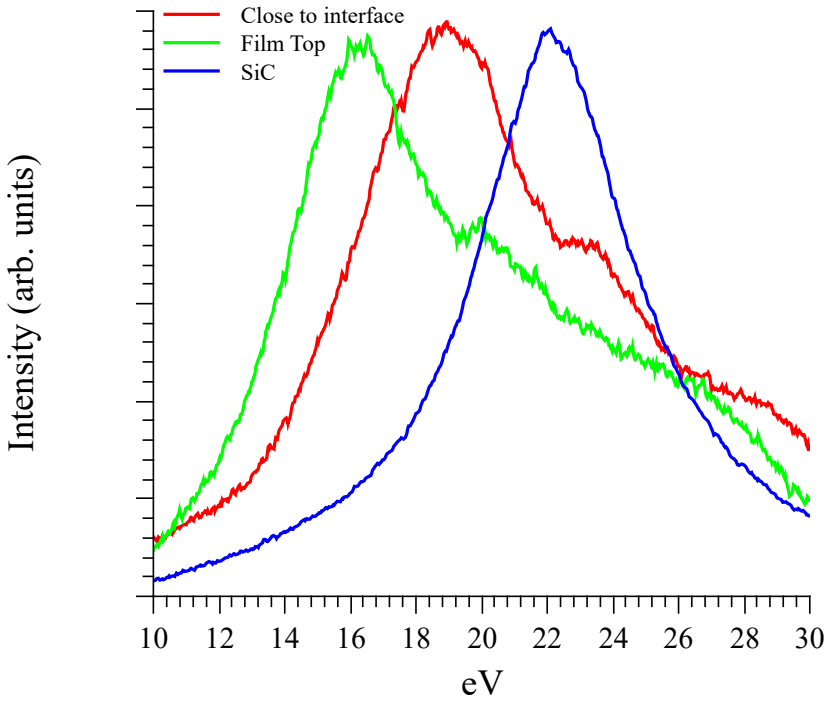

Figure S6: *Plasmon peaks from low-loss EELS spectra of the SiC substrate and the epitaxial $In_xGa_{1-x}N$ deposited at 350 °C from a 1:1 powder ratio of **1** and **2** sublimed at 130 °C.*

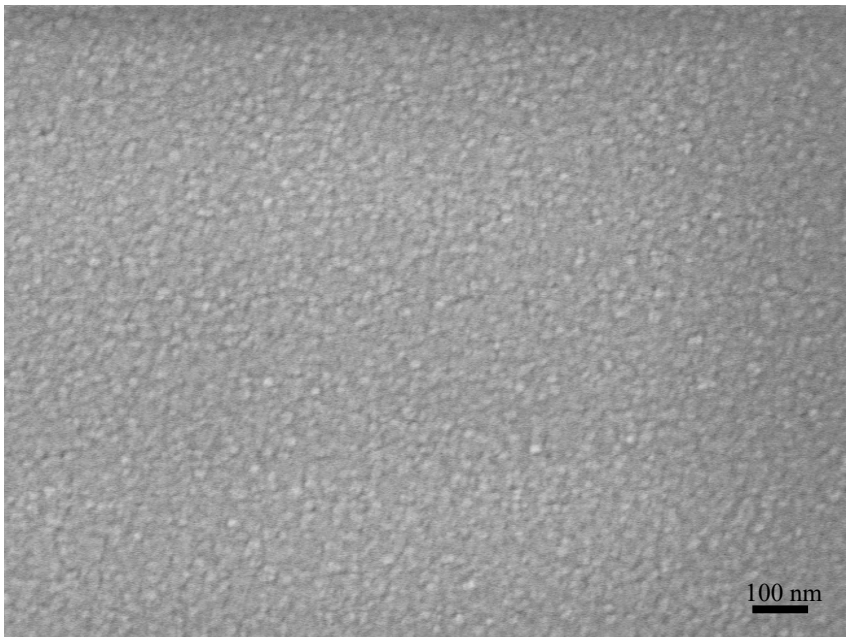

Figure S7: *Top-view SEM measurement of 60 nm thick InGaN deposited at 350 °C with a bubbler temperature of 150 °C on Si (100) substrate.*

References

1 N. J. O'Brien, P. Rouf, R. Samii, K. Rönnby, S. C. Buttera, C. W. Hsu, I. G. Ivanov, V. Kessler, L. Ojamäe and H. Pedersen, *Chem. Mater.*, 2020, **32**, 4481–4489.

2 P. Rouf, R. Samii, K. Rönnby, B. Bakhit, S. C. Buttera, I. Martinovic, L. Ojamäe, C. W. Hsu, J. Palisaitis, V. Kessler, H. Pedersen and N. J. O'Brien, *Chem. Mater.*, 2021, **33**, 3266–3275.

3 M. Mayer, W. Eckstein, H. Langhuth, F. Schiettekatte and U. Von Toussaint, *Nucl. Instruments Methods Phys. Res. Sect. B Beam Interact. with Mater. Atoms*, 2011, **269**, 3006–3013.

4 P. Ström, P. Petersson, M. Rubel and G. Possnert, *Rev. Sci. Instrum.*, 2016, **87**, 103303.

5 K.S. Janson, 2004.

6 K. Arstila, J. Julin, M. I. Laitinen, J. Aalto, T. Konu, S. Kärkkäinen, S. Rahkonen, M. Raunio, J. Itkonen, J. P. Santanen, T. Tuovinen and T. Sajavaara, *Nucl. Instruments Methods Phys. Res. Sect. B Beam Interact. with Mater. Atoms*, 2014, **331**, 34–41.

7 Y. Zhang, H. J. Whitlow, T. Winzell, I. F. Bubb, T. Sajavaara, K. Arstila and J. Keinonen, *Nucl. Instruments Methods Phys. Res. Sect. B Beam Interact. with Mater. Atoms*, 1999, **149**, 477–489.

8 M. A. Arvizu, R. T. Wen, D. Primetzhofer, J. E. Klemberg-Sapieha, L. Martinu, G. A. Niklasson and C. G. Granqvist, *ACS Appl. Mater. Interfaces*, 2015, **7**, 26387–26390.

9 H. Y. Qu, D. Primetzhofer, M. A. Arvizu, Z. Qiu, U. Cindemir, C. G. Granqvist and G. A. Niklasson, *ACS Appl. Mater. Interfaces*, 2017, **9**, 42420–42424.

10 J. F. Ziegler, M. D. Ziegler and J. P. Biersack, *Nucl. Instruments Methods Phys. Res. Sect. B Beam Interact. with Mater. Atoms*, 2010, **268**, 1818–1823.

11 P. Rouf, N. J. O'Brien, S. C. Buttera, I. Martinovic, B. Bakhit, E. Martinsson, J. Palisaitis, C. W. Hsu and H. Pedersen, *J. Mater. Chem. C*, 2020, **8**, 8457–8465.

12 S. Krischok, V. Yanev, O. Balykov, M. Himmerlich, J. A. Schaefer, R. Kosiba, G. Ecke, I. Cimalla, V. Cimalla, O. Ambacher, H. Lu, W. J. Schaff and L. F. Eastman, *Surf. Sci.*, 2004, **566**–**568**, 849–855.

13 J. Palisaitis, A. Lundskog, U. Forsberg, E. Janzén, J. Birch, L. Hultman and P. O. A. Persson, *J. Appl. Phys.*, 2014, **115**, 034302.

14 J. Palisaitis, C. L. Hsiao, M. Junaid, M. Xie, V. Darakchieva, J. F. Carlin, N. Grandjean, J. Birch, L. Hultman and P. O. . Persson, *Phys. Status Solidi - Rapid Res. Lett.*, 2011, **5**, 50–52.